Eur. Phys. J. D (2016) 70: 224
DOI: 10.1140/epjd/e2016-70225-3

THE EUROPEAN PHYSICAL JOURNAL D

Regular Article

Effect of circularly polarized femtosecond laser pulses on alignment dynamics of linear molecules observed by strong-field photoelectron yields

Necati Kaya[1,2,3,a], Gamze Kaya[1,2], James Strohaber[4], Alexandre A. Kolomenskii[1], and Hans A. Schuessler[1,2]

[1] Department of Physics, Texas A&M University, College Station, 77843 Texas, USA
[2] Science Program, Texas A&M University at Qatar, 23874 Doha, Qatar
[3] Department of Physics, Giresun University, 28200 Giresun, Turkey
[4] Department of Physics, Florida Agricultural and Mechanical University, Tallahassee, 32307 Florida, USA

Received 29 March 2016 / Received in final form 10 August 2016
Published online 25 October 2016 – © EDP Sciences, Società Italiana di Fisica, Springer-Verlag 2016

Abstract. By measuring femtosecond laser driven strong-field electron yields for linear molecules aligned by circularly polarized femtosecond laser pulses, we study the rotational wavepacket evolution of N_2, CO, and C_2H_2 gas molecules. We show that circular polarization produces a net alignment along the laser pulse propagation axis at certain phases of the evolution. This gives the possibility to control alignment of linear molecules outside the plane of polarization, which can provide new capabilities for molecular imaging. The experimental results were compared to the calculated field-free molecular alignment parameter taking into account the effects of electronic structure and symmetry of the molecules. By fitting the calculated impulsive alignment parameter to the measured experimental data we determined the molecular rotational constants of the linear gas molecules.

1 Introduction

The studies of intense laser field interaction with molecules have attracted increasing attention due to additional features of molecules in comparison to atoms, e.g. molecular orientation, orbital symmetry, internuclear distances, etc. [1–5]. A molecule with an anisotropic polarizability exposed to a strong linearly polarized laser field creates an induced dipole moment, and the molecule leans towards the state with its most polarizable axis along the laser polarization direction [6]. A short laser pulse (much shorter than the molecular rotational period) aligns the molecules nonadiabatically, and the alignment exhibits periodic revivals after the laser pulse has ended [3,7,8]. Femtosecond laser technology allows aligning molecules and observing molecular dynamics by using a pump-probe technique, where a pump pulse initiates alignment by creating a dynamically anisotropic medium evolving in time. The variations of the interaction with such a medium with a delayed probe pulse can be observed by ionization [9–11], fragmentation [12–15] or high harmonic generation [16–23].

While linearly polarized laser pulse aligns the most polarizable molecular axis in the laser field polarization direction [3], a pulse with elliptical polarization creates planar alignment of the large and small polarizability axes of asymmetric top molecules [14,24–26]. In the plane of polarization molecular alignment can be controlled by both linear and elliptically polarized aligning pulses [27]. However, for many applications, it is important to align molecules outside the plane of polarization [28], which can be achieved by circularly polarized probe pulses and is studied in this paper.

The circularly polarized aligning pulse produces a torque on the molecules by pulling the most polarizable axis into the plane of polarization. This creates a rotational wave packet that re-aligns under field-free conditions to the plane of polarization every revival period [3]. For a linear molecule, just before the revival, the molecular axis first aligns along the direction of laser propagation, which is called "k-alignment" [27], then the molecule keeps rotating, and in a short time later the molecular axis is aligned with the field polarization plane.

For aligning the linear molecules N_2, CO, and C_2H_2, we used a circularly polarized femtosecond pulse to control molecular alignment outside the plane of polarization. We measured femtosecond laser driven strong-field ionization yields of photoelectrons from aligned linear molecules. The impulsive molecular alignment by circularly polarized laser pulses was also calculated and compared to the experimental results, which were discussed taking into account the effects of the electronic structure and symmetry of the molecules. Then by fitting the calculated impulsive alignment parameter to the measured experimental data, we determined the molecular rotational constants of the molecules.

[a] e-mail: necati@physics.tamu.edu

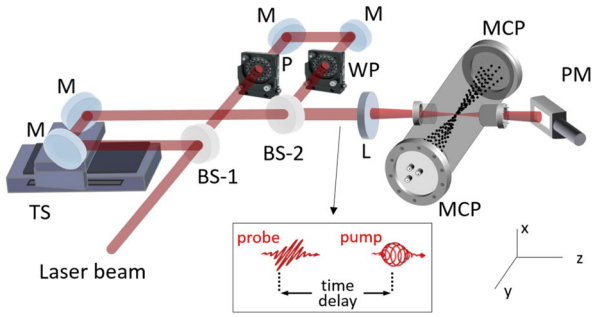

Fig. 1. Experimental setup. BS: beam-splitters, TS: translational stage, WP: wave plates, M: flat mirrors, L: achromatic focusing lens, PM: power meter, MCP: microchannel plates. The electrons ionized in the focal region fly toward MCP detectors for registration.

2 Experimental details

We used our pump-probe setup with the above threshold ionization (ATI) apparatus as shown in Figure 1 [29] to create impulsive molecular alignment and to monitor its dynamics via the measured total electron yield from strong-field ionization. In our experiments, ultrashort pulses were produced by a regenerative laser amplifier, which outputs 56 fs (measured by frequency resolved optical gating, GRENOUILLE 8–20, Swamp Optics, LLC) laser pulses at a repetition rate of 1 kHz and with the central wavelength of 800 nm. The input pulse was split by a beam-splitter into two beams as pump and probe pulses with typical intensities of 2×10^{13} W/cm^2 and 8.8×10^{13} W/cm^2, respectively. A combination of a polarizer and a quarter-wave plate placed into the pump arm assured the proper circular polarization and power of the pump pulse. The delay of the pump and probe pulses was precisely adjusted using an optical time delay variable with a stepping-motor-controlled translational stage (Newport, Model 301) having the high resolution of 0.66 fs. The combined beams were focused by a 20 cm achromatic lens into the vacuum chamber. One of the gases (N_2, CO, or C_2H_2 from Matheson TRIGAS, with purities of 99.9995%, 99.9%, 99.997%, 99.6%, respectively) was admitted through an adjustable leak valve into the vacuum chamber. The circularly polarized pump pulse creates rotational wave packets, and then the probe pulse, which is linearly polarized along the axis connecting the centers of the microchannel plate (MCP) detectors and has an adjustable time delay, ionizes molecules in the laser focal region. Electrons ejected along the polarization of the probe laser field then travel inside a μ-metal TOF tube in a field-free region and are registered by the MCP detectors. The signals from the MCP detectors were preamplified (ZKL-2 Mini-Circuits) and then registered by a fast ComTech MCS6 multiple-event time digitizer with 100 ps time resolution. The total number of photoelectron counts formed the measured output signal that depended on the pump-probe delay. To reduce the effect of variations of the laser power during the experiment, a power meter was placed at the exit window of the chamber, and the electron yields were normalized to the measured laser power. During the experiment, the strong-field ionization yields at variable pump-probe time delays are measured, which reveals the rotational wavepacket evolution, including the events of planar alignment (the rotational wavepacket aligning to the plane of polarization) and k-alignment (the rotational wavepacket aligning along the direction of the pump pulse propagation).

3 Impulsive molecular alignment by circularly polarized laser pulses

The nonresonant dipole potential for circular polarization induced by an electric field $E(t)$ is $V_C(t) = -1/2\alpha_C E^2(t)$, where α_C is the effective polarizability for a circularly polarized light, and can be derived in the following way [30,31]. The alignment of the molecule is described in spherical coordinates and we choose the Z axis parallel to the propagation direction of the circularly polarized light. For circularly polarized light, the induced dipole moment is $\mu = \mu_X^{ind}\hat{i} + \mu_Y^{ind}\hat{j}$ with

$$\mu_X^{ind} = \left(\alpha_{xx}\Lambda_{Xx}^2 + \alpha_{yy}\Lambda_{Xy}^2 + \alpha_{zz}\Lambda_{Xz}^2\right) E_X$$

and

$$\mu_Y^{ind} = \left(\alpha_{xx}\Lambda_{Yx}^2 + \alpha_{yy}\Lambda_{Yy}^2 + \alpha_{zz}\Lambda_{Yz}^2\right) E_Y,$$

where Λ_{Gg} are determined by Euler rotation angles for the lab fixed axis G and the body fixed axis g. The effective polarizability for $|E_X| = |E_Y| = E$ is

$$\frac{\mu_X^{ind} + \mu_Y^{ind}}{E} = \alpha_\perp \left(\Lambda_{Xx}^2 + \Lambda_{Xy}^2 + \Lambda_{Yx}^2 + \Lambda_{Yy}^2\right) + \alpha_{||} \left(\Lambda_{Xz}^2 + \Lambda_{Yz}^2\right).$$

By using $\sum_g \Lambda_{Zg}^2 = 1$ and $\sum_G \Lambda_{Gz}^2 = 1$ [32], the effective polarizability can be written as $\alpha = 1/2[\alpha_\perp(1 + \cos^2\theta) + \alpha_{||}\sin^2\theta]$, where θ is the angle between the molecular axis and the field propagation direction of the aligning pulse. For the complete alignment of a molecule in a circularly polarized laser field $\theta = 90°$, and the maximum effective polarizability is $\alpha = (\alpha_{||} + \alpha_\perp)/2$, whereas for the complete anti-alignment, $\theta = 0$, and the minimum effective polarizability is $\alpha = \alpha_\perp$. The expression of the nonresonant dipole potential for circular polarization becomes $V(t) = -1/4(\alpha_{||} + \alpha_\perp - \Delta\alpha\cos^2\theta)E^2(t)$ [33–35], where $\Delta\alpha = \alpha_{||} - \alpha_\perp$ is the polarizability difference between the components parallel $\alpha_{||}$ and perpendicular $\alpha_\perp$ to the molecular axis. The interaction of a linearly polarized pump pulse with linear molecules can be described by the effective Hamiltonian $H = H_0 - 1/4(\alpha_{||} + \alpha_\perp - \Delta\alpha\cos^2\theta)E^2(t)$, where $H_0 = B\hat{J}^2$ is field free Hamiltonian with the rotational molecular constant B and the angular momentum operator $\hat{J}$; $E(t)$ is the amplitude of the aligning pulse.

The degree of molecular alignment is characterized by the quantity $\langle\langle\cos^2\theta\rangle\rangle$, calculated by a double averaging procedure. In the first step of averaging

over rotational states, each molecular rotational state $|\Phi_{J_0M_0(t)}\rangle = \sum_{JM} d_{JM}^{J_0M_0}(t)\exp(-iE_Jt/\hbar)|JM\rangle$ and its amplitudes $d_{JM}^{J_0M_0}(t)$ are found by solving the Schrödinger equation in terms of field-free rotor functions $|JM\rangle$ with eigen energy $E_J = hBcJ(J+1)$ [3,36,37]. Then the degree of molecular alignment at time t is obtained as $\langle\cos^2\theta\rangle_{J_0M_0}(t) = \langle\Phi_{J_0M_0}(t)|\cos^2\theta|\Phi_{J_0M_0}(t)\rangle$ [8]. This expression can be written more explicitly by using the time-dependent phase terms $|\Phi_{J_0M_0}(\tau)\rangle = \sum_{J,M} d_{JM}|JM\rangle\exp[-i\pi J(J+1)\tau]$ [38] and introducing time τ in units of $T_{rev} = 1/(2Bc)$. Consequently,

$$\begin{aligned}\langle\cos^2\theta\rangle_{J_0M_0}(\tau) &= \langle\Phi_{J_0M_0}(\tau)|\cos^2\theta\,|\Phi_{J_0M_0}(\tau)\rangle \\ &= \sum_{J',M'}\sum_{J,M} d^*_{J'M'}d_{JM}\,\langle J'M'| \\ &\quad\times\cos^2\theta\,|JM\rangle\,\varphi_{J,J'},\end{aligned} \tag{1}$$

where selection rules for the rotational transitions require $\langle J'M'|\cos^2\theta|JM\rangle \propto \delta_{\left\{\begin{smallmatrix}J,J'\\J,J'\pm2\end{smallmatrix}\right\}}\delta_{M,M'}$ [8] and the phase factors are $\varphi_{J,J'} = \exp(-i\pi\tau[J'(J'+1) - J(J+1)])$. For the terms with the same angular momentum quantum number, $J = J'$, the time-dependent phase disappears, but for the terms of $J = J' \pm 2$, the time dependence is given by the phase factors: $\varphi_{J,J\pm2} = \exp[-i\pi\tau(4J+6)]$. Often the molecular ionization rate is maximal when the maximum of the initial electron density corresponds to the laser polarization direction of the applied field. However, not all diatomic molecules have their highest occupied molecular orbital (HOMO), which donates electrons most readily, lined up along the molecular axis. For example, for π electrons, this orbit is preferentially aligned in the direction perpendicular to the molecular axis with no electron density on the internuclear axis, while for σ electrons, it is preferentially aligned in the direction parallel to the molecular (internuclear) axis due to the shared electron density directly between the bonding atoms. Therefore, depending on the configuration of the HOMO orbital, qualitatively different alignment signatures can be expected based on the detection of strong-field ionization yields in the interaction of the aligned molecules with the probe pulse. Thus, we should add an additional term to the phase factor: $\varphi'_{J,J\pm2} = \exp[-i(\pi\tau(4J+6)+\Delta)]$, where Δ is determined from the configuration of the HOMO orbital in agreement with the alignment signatures following from the observed strong-field ionization yields in the interaction of the aligned molecules with the probe pulse.

In the second step, averaging is performed over initial states, which are assumed to be populated according to the temperature dependent Boltzmann distribution. The resultant degree of molecular alignment can then be presented as [39]

$$\langle\langle\cos^2\theta\rangle\rangle = \frac{\sum_{J_0} Q_{J_0}\sum_{M_0=-J_0}^{J_0}\langle\cos^2\theta\rangle_{J_0M_0}}{\sum_{J_0} Q_{J_0}}, \tag{2}$$

where

$$Q_{J_0} \approx g_{J_0}(2J_0+1)\exp[-BJ_0(J_0+1)/kT]$$

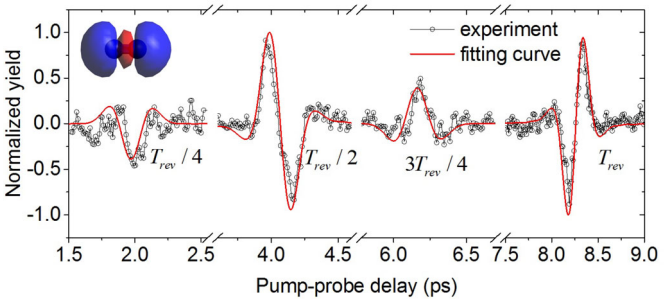

Fig. 2. Strong-field ionization yield of impulsively aligned nitrogen gas molecules along with the fitting curve as a function of the pump-probe delay.

is the population probability of state J_0. The $(2J_0+1)$ term accounts for the degeneracy within a given J_0 state. In the case of a molecule containing two identical nuclei, g_{J_0} is the relative weight between odd and even J states, which comes from nuclear spin statistics as an additional factor [40,41].

4 Results and discussions

In Figure 2 we present the measured strong-field ionization yield for N_2 molecules aligned by a circularly polarized pump pulse and the corresponding fitting curve based on the degree of molecular alignment $\langle\langle\cos^2\theta\rangle\rangle$. A temperature $T = 300$ K is assumed in the fitting functions. These dependences are shown as functions of the delay after the action of the pump pulse, i.e. pump-probe delay. We observed strong alignment effects at multiples of $T_{rev}/2$ and the signals at odd multiples of $T_{rev}/4$ with reduced amplitudes due to the ratio of even:odd =2:1 for the nuclear spin-statistical factors of N_2 [29,42,43]. From the fitting function, we found $\Delta = 0$ for N_2 measurements. This means that the molecular ionization rate is maximal when molecules are aligned along the laser polarization direction, and the configuration of the HOMO orbital is parallel to the molecular axis, because such configuration makes ejection of an electron easier. As seen in the inset of Figure 2, N_2 has the maximum electron density along the internuclear (molecular) axis due to its σ_g HOMO. By fitting the curve, we also evaluated the characteristic rotational constant of nitrogen gas to be 2.0134 cm^{-1} and the corresponding revival time to be 8.283 ps.

For CO, which contains nonidentical nuclei, there is no additional factor arising from the nuclear spin statistics [41,44]. Thus, the revivals at odd multiples of $T_{rev}/4$ are completely cancelled, whereas only the revivals at multiples of $T_{rev}/2$ remain, as presented in Figure 3. From the fitting function, we found $\Delta = 0$ for CO, which is similar to the N_2 measurements. CO has σ HOMOs, so there is no nodal plane along the internuclear axis, and therefore the calculated time dependency of molecular alignment is in phase with the measured strong-field photoelectron yield. For CO, we calculated the characteristic rotational constant as 1.9553 cm^{-1}, and the corresponding revival period is 8.529 ps.

Table 1. Experimental and theoretical molecular rotational constants and corresponding molecular revival periods.

	Rotational constants (cm^{-1})		Full revival period (ps)	
	Experimental	Theoretical	Experimental	Theoretical
N_2	2.0134	1.9896	8.283	8.383
CO	1.9553	1.9313	8.539	8.636
C_2H_2	1.1898	1.1766	14.017	14.175

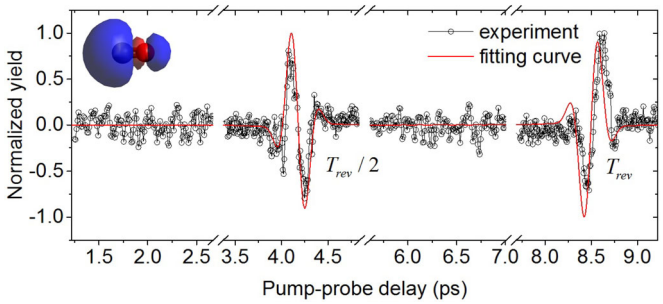

Fig. 3. Strong-field ionization yield of impulsively aligned CO gas molecules along with the fitting curve.

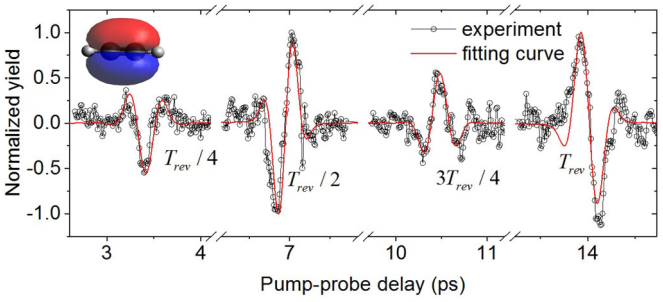

Fig. 4. Strong-field ionization yields of impulsive aligned C_2H_2 gas molecules along with the fitting curve.

Discussing results for C_2H_2, we note that this molecule has both odd and even J-states, which are populated with the ratio of odd J-states to even J-states 3:1 [45]. Because of this fact, even and odd wave packets partially cancel each other, and some alignment and anti-alignment are observed at quarter revivals, as seen in Figure 4. From the fitting function, we found $\Delta = \pi$, which gives a reversed signal structure of the molecular alignment parameter$\langle\langle\cos^2\theta\rangle\rangle$. This can be understood from the HOMO of acetylene, which is dominated by a π_u orbital [46]. Indeed, π_u molecular orbitals have electron density surrounding the bond axis (increased electron density above/below internuclear axis) with a node along the internuclear axis, as shown in the inset of Figure 4. For C_2H_2, we evaluated the characteristic rotational constant as 1.1898 cm^{-1} and corresponding periodic revival time is 14.017 ps.

The characteristic molecular rotational constants and corresponding periods of revivals evaluated from fitting the parameter of the degree of molecular alignment (see Eq. (2)) of the ensemble of molecules for each investigated molecule in comparison to the theoretical values [6,44,47,48] are presented in Table 1.

5 Conclusions

In conclusion, for the linear molecules N_2, CO, and C_2H_2 we observed the revival signatures produced by circularly polarized pump pulses at the conditions of impulsive alignment using detection of photoelectrons produced in strong-field ionization by a variably delayed probe pulse. The ability of controlling the alignment of linear molecules outside the plane of polarization can open new capabilities for molecular imaging. The presented treatment is for linear molecules only and could be extended to the more general case, which has been extensively investigated as well, including 3D alignment (see, for instance Ref. [49]). By fitting the calculated parameter of the degree of molecular alignment $\langle\langle\cos^2\theta\rangle\rangle$ to the experimental data, we determined the values of the molecular rotational constants and revival periods, which are in good agreement with the theoretical literature values. The effects of the electronic structure and symmetry of molecules on the signatures of the alignment revivals are discussed and show that for N_2 and CO the strong-field ionization yields change similarly to the degree of molecular alignment, while for C_2H_2 the changes of the strong-field ionization yield are reversed in sign as compared to the variations of the degree of molecular alignment.

Author Contribution Statement

N.K. and G.K. designed the experimental setup and performed all of the experiments. N.K., G.K., and A.A.K. interpreted the results and N.K. wrote the draft manuscript. J.S., A.A.K. and H.A.S. supervised the progress of work, data interpretation and preparation and editing of the manuscript.

This work was supported by the Robert A. Welch Foundation Grant No. A1546, and the Qatar Foundation under the grant NPRP 6-465-1-091.

References

1. A.D. Bandrauk, *Molecules in Laser Fields* (Marcel Dekker, New York, 1994)
2. J.H. Posthumus, Rep. Progress Phys. **67**, 623 (2004)
3. H. Stapelfeldt, T. Seideman, Rev. Mod. Phys. **75**, 543 (2003)
4. X. Lai, C.F.d.M. Faria, Phys. Rev. A **88**, 013406 (2013)
5. Z. Hu, X. Lai, X. Liu, J. Chen, Phys. Rev. A **89**, 043401 (2014)

6. N. Xu, J. Li, J. Li, Z. Zhang, Q. Fan, in *Lasers – Applications in Science and Industry*, edited by K. Jakubczak (2011)
7. T. Seideman, J. Chem. Phys. **103**, 7887 (1995)
8. J. Ortigoso, M. Rodríguez, M. Gupta, B. Friedrich, J. Chem. Phys. **110**, 3870 (1999)
9. V. Loriot, E. Hertz, B. Lavorel, O. Faucher, J. Phys. B: At. Mol. Opt. Phys. **41**, 015604 (2008)
10. D. Pavičić, K.F. Lee, D.M. Rayner, P.B. Corkum, D.M. Villeneuve, Phys. Rev. Lett. **98**, 243001 (2007)
11. I.V. Litvinyuk, K.F. Lee, P.W. Dooley, D.M. Rayner, D.M. Villeneuve, P.B. Corkum, Phys. Rev. Lett. **90**, 233003 (2003)
12. E. Péronne, M.D. Poulsen, C.Z. Bisgaard, H. Stapelfeldt, T. Seideman, Phys. Rev. Lett. **91**, 043003 (2003)
13. M. Kenzo, S. Takayuki, N. Didier, J. Phys. B: At. Mol. Opt. Phys. **37**, 753 (2004)
14. I. Nevo, L. Holmegaard, J.H. Nielsen, J.L. Hansen, H. Stapelfeldt, F. Filsinger, G. Meijer, J. Kupper, Phys. Chem. Chem. Phys. **11**, 9912 (2009)
15. P.W. Dooley, I.V. Litvinyuk, K.F. Lee, D.M. Rayner, M. Spanner, D.M. Villeneuve, P.B. Corkum, Phys. Rev. A **68**, 023406 (2003)
16. R. Velotta, N. Hay, M.B. Mason, M. Castillejo, J.P. Marangos, Phys. Rev. Lett. **87**, 183901 (2001)
17. N. Hay, R. Velotta, M. Lein, R. de Nalda, E. Heesel, M. Castillejo, J.P. Marangos, Phys. Rev. A **65**, 053805 (2002)
18. J. Itatani, J. Levesque, D. Zeidler, H. Niikura, H. Pépin, J.C. Kieffer, P.B. Corkum, D.M. Villeneuve, Nature **432**, 867 (2004)
19. T. Kanai, S. Minemoto, H. Sakai, Nature **435**, 470 (2005)
20. C. Vozzi, F. Calegari, E. Benedetti, J.P. Caumes, G. Sansone, S. Stagira, M. Nisoli, R. Torres, E. Heesel, N. Kajumba, J.P. Marangos, C. Altucci, R. Velotta, Phys. Rev. Lett. **95**, 153902 (2005)
21. J.P. Marangos, S. Baker, N. Kajumba, J.S. Robinson, J.W.G. Tisch, R. Torres, Phys. Chem. Chem. Phys. **10**, 35 (2008)
22. D. Shafir, Y. Mairesse, D.M. Villeneuve, P.B. Corkum, N. Dudovich, Nat. Phys. **5**, 412 (2009)
23. B.K. McFarland, J.P. Farrell, P.H. Bucksbaum, M. Gühr, Science **322**, 1232 (2008)
24. J.J. Larsen, K. Hald, N. Bjerre, H. Stapelfeldt, T. Seideman, Phys. Rev. Lett. **85**, 2470 (2000)
25. J.L. Hansen, H. Stapelfeldt, D. Dimitrovski, M. Abu-samha, C.P.J. Martiny, L.B. Madsen, Phys. Rev. Lett. **106**, 073001 (2011)
26. D. Dimitrovski, M. Abu-samha, L.B. Madsen, F. Filsinger, G. Meijer, J. Küpper, L. Holmegaard, L. Kalhøj, J.H. Nielsen, H. Stapelfeldt, Phys. Rev. A **83**, 023405 (2011)
27. C.T.L. Smeenk, P.B. Corkum, J. Phys. B **46**, 201001 (2013)
28. C.T.L. Smeenk, L. Arissian, A.V. Sokolov, M. Spanner, K.F. Lee, A. Staudte, D.M. Villeneuve, P.B. Corkum, Phys. Rev. Lett. **112**, 253001 (2014)
29. N. Kaya, G. Kaya, M. Sayrac, Y. Boran, S. Anumula, J. Strohaber, A.A. Kolomenskii, H.A. Schuessler, Opt. Express **24**, 2562 (2016)
30. B.J. Sussman, J.G. Underwood, R. Lausten, M.Y. Ivanov, A. Stolow, Phys. Rev. A **73**, 053403 (2006)
31. B.W. Shore, *The Theory of Coherent Atomic Excitation, Multilevel Atoms and Incoherence* (Wiley, 1990)
32. S.M. Purcell, *UCL* (University College London, 2010)
33. T. Seideman, J. Chem. Phys. **107**, 10420 (1997)
34. J.D. Graybeal, *Molecular spectroscopy* (McGraw-Hill, 1988)
35. S.M. Purcell, P.F. Barker, Phys. Rev. Lett. **103**, 153001 (2009)
36. F.H.M. Faisal, A. Abdurrouf, Phys. Rev. Lett. **100**, 123005 (2008)
37. P.F. Bernath, P.F. Bernath, *Spectra of Atoms and Molecules* (Oxford University Press, New York, 1995)
38. S. Fleischer, Y. Khodorkovsky, E. Gershnabel, Y. Prior, I.S. Averbukh, Israel J. Chem. **52**, 414 (2012)
39. H. Zeng, P. Lu, J. Liu, W. Li, in *Progress in Ultrafast Intense Laser Science VIII*, edited by K. Yamanouchi, M. Nisoli, T.W. Hill (Springer Berlin Heidelberg, Berlin, Heidelberg, 2012), p. 47
40. B.H. Bransden, C.J. Joachain, *Physics of Atoms and Molecules* (Prentice Hall, 2003)
41. D.A. McQuarrie, J.D. Simon, *Physical Chemistry: A Molecular Approach* (University Science Books, 1997)
42. S. Fleischer, I.S. Averbukh, Y. Prior, Phys. Rev. A **74**, 041403 (2006)
43. P. Atkins, J. de Paula, R. Friedman, *Quanta, Matter, and Change: A Molecular Approach to Physical Chemistry* (OUP Oxford, 2009)
44. R.B. Philip, J. Per, *Molecular Symmetry and Spectroscopy*, 2nd edn. (NRC Research Press, 2006)
45. H. Li, W. Li, Y. Feng, J. Liu, H. Pan, H. Zeng, Phys. Rev. A **85**, 052515 (2012)
46. R. Torres, N. Kajumba, J.G. Underwood, J.S. Robinson, S. Baker, J.W.G. Tisch, R. de Nalda, W.A. Bryan, R. Velotta, C. Altucci, I.C.E. Turcu, J.P. Marangos, Phys. Rev. Lett. **98**, 203007 (2007)
47. W.M.L.D.R. Haynes, *CRC handbook of chemistry and physics: a ready-reference book of chemical and physical data* (CRC Press Boca Raton, Fla., 2011)
48. M. Herman, A. Campargue, M.I. El Idrissi, J. Vander Auwera, J. Phys. Chem. Reference Data **32**, 921 (2003)
49. J.G. Underwood, B.J. Sussman, A. Stolow, Phys. Rev. Lett. **94**, 143002 (2005)